The haloes of bright satellite galaxies in a warm dark matter universe

Mark R. Lovell,[1]* Vincent Eke,[1] Carlos S. Frenk,[1] Liang Gao,[1,2] Adrian Jenkins,[1] Tom Theuns,[1,3] Jie Wang,[1] Simon D. M. White,[4] Alexey Boyarsky[5,6] and Oleg Ruchayskiy[7]

[1]*Institute for Computational Cosmology, Durham University, South Road, Durham DH1 3LE*
[2]*National Astronomical Observatories, Chinese Academy of Science, Beijing 100012, China*
[3]*Department of Physics, University of Antwerp, Groenenborgerlaan 171, B-2020 Antwerpen, Belgium*
[4]*Max-Planck-Institut für Astrophysik, Karl-Schwarzschild-Straße 1, 85740 Garching bei München, Germany*
[5]*École Polytechnique Fédérale de Lausanne, FSB/ITP/LPPC, BSP 720, CH-1015 Lausanne, Switzerland*
[6]*Bogolyubov Institute of Theoretical Physics, Kiev 03680, Ukraine*
[7]*CERN Physics Department, Theory Division, CH-1211 Geneva 23, Switzerland*

ABSTRACT

High-resolution *N*-body simulations of galactic cold dark matter haloes indicate that we should expect to find a few satellite galaxies around the Milky Way whose haloes have a maximum circular velocity in excess of $40 \, \mathrm{km \, s^{-1}}$. Yet, with the exception of the Magellanic Clouds and the Sagittarius dwarf, which likely reside in subhaloes with significantly larger velocities than this, the bright satellites of the Milky Way all appear to reside in subhaloes with maximum circular velocities below $40 \, \mathrm{km \, s^{-1}}$. As recently highlighted by Boylan-Kolchin et al., this discrepancy implies that the majority of the most massive subhaloes within a cold dark matter galactic halo are too concentrated to be consistent with the kinematic data for the bright Milky Way satellites. Here we show that no such discrepancy exists if haloes are made of warm rather than cold dark matter because these haloes are less concentrated on account of their typically later formation epochs. Warm dark matter is one of several possible explanations for the observed kinematics of the satellites.

Key words: galaxies: dwarf – dark matter.

1 INTRODUCTION

Measurements of temperature anisotropies in the microwave background radiation (e.g. Komatsu et al. 2011) of galaxy clustering on large scales (e.g. Cole et al. 2005), and of the currently accelerated expansion of the Universe (e.g. Clocchiatti et al. 2006; Guy et al. 2010) have confirmed the 'Λ cold dark matter' (ΛCDM) model, first explored theoretically 25 years ago (Davis et al. 1985), as the standard model of cosmogony. These observations probe a large range of scales, from ∼1 Gpc to ∼10 Mpc. On smaller scales, where the distribution of dark matter is strongly non-linear, observational tests of the model are more complicated because of the complexity added by galaxy formation processes. However, it is precisely on these scales that the nature of the dark matter may be most clearly manifest. For example, if the dark matter is made of warm rather than cold particles, free streaming in the early universe would have erased primordial fluctuations below a scale that depends on the mass of the dark matter particle, but could be of order 10^9–$10^{10} \, \mathrm{M_\odot}$. These mass scales correspond to dwarf galaxies and

so, in principle, the abundance and properties of dwarf galaxies could encode information about the nature of the dark matter.

The validity of the ΛCDM model on galactic and subgalactic scales has been a subject of debate for many years. Initially Klypin et al. (1999) and Moore et al. (1999) pointed out a large discrepancy between the number of dark matter substructures, or subhaloes, that survive inside a galactic halo and the number of satellites that are observed around the Milky Way. This so-called 'satellite problem' is often interpreted as indicating that the model requires most of the subhaloes to contain no visible satellite. This aspect of the problem, however, is readily solved by invoking the known physics of galaxy formation, particularly early reionization of the intergalactic medium and supernovae feedback, which inevitably inhibit the formation of stars in small-mass haloes. Detailed models that reconcile theory and observations in this way date back to the early 2000s (Bullock, Kravtsov & Weinberg 2000; Benson et al. 2002; Somerville 2002).

The paucity of observed bright satellites, however, is only one aspect of the satellite problem. As already emphasized by Klypin et al. (1999) and Moore et al. (1999), there is a problem not only with the abundance of satellites, but also with their distribution of circular velocities. In a halo like that of the Milky Way, the ΛCDM model

*E-mail: m.r.lovell@durham.ac.uk

predicts the existence of several subhaloes with maximum circular velocities, V_{max},[1] in excess of $\sim$40 km s^{-1}. Using the high-resolution simulations of galactic haloes of the Aquarius project (Springel et al. 2008), Strigari, Frenk & White (2010) have recently demonstrated that it is possible to find ΛCDM subhaloes that accurately match the observed stellar kinematics of the five well-studied satellites of the Milky Way. The best fits, however, invariably have $V_{max} \lesssim$ 40 km s^{-1}. [The Strigari et al. sample excludes the Large and Small Magellanic Clouds (LMC and SMC) which reside in more massive haloes, and Sagittarius which is currently being disrupted.]

The discrepancy between the predicted and inferred distributions of V_{max} values has recently been highlighted by Boylan-Kolchin, Bullock & Kaplinghat (2011). Using also the Aquarius haloes, as well as the Via Lactea simulations (Madau, Diemand & Kuhlen 2008), they show explicitly that the simulated haloes typically contain a few subhaloes which are too massive and too dense (as indicated by their value of V_{max}/r_{max}) to host any of the observed satellites. If such objects existed in the Milky Way, they would have to be empty of stars despite their mass. This seems very unlikely so, unless the Milky Way is atypical, there is an apparent discrepancy between model and observations.

That the Milky Way is not typical of isolated galaxies of similar luminosity and colour has recently been established from Sloan Digital Sky Survey data. Liu et al. (2011) have shown that only 3.5 per cent of such galaxies have two satellites as bright as the Magellanic Clouds, while Guo et al. (2011) have shown that the luminosity function of the bright ($M_V < -14$) Milky Way satellites has about twice the amplitude of the mean for similar galaxies (see also Lares, Lambas & Domínguez 2011). While these measurements show that the Milky Way is not an average galaxy, it is not at present possible to compare the distribution of V_{max} of its satellites with that of similar galaxies directly. However, an indirect probe of this distribution can be constructed by combining N-body simulations with a subhalo abundance matching procedure (Busha et al. 2011).

In this paper we explore whether an alternative hypothesis for the nature of the dark matter, a warm rather than a cold particle, can provide a better match to the inferred distribution of satellite circular velocities or masses. Specifically, we test a model in which the dark matter is one of the particles predicted by the 'neutrino minimal standard model (νMSM)' of Asaka & Shaposhnikov (2005) and Boyarsky, Ruchayskiy & Shaposhnikov (2009a). In this model there is a triplet of sterile neutrinos, the lightest of which could become non-relativistic at a redshift of $\sim$10^6, have a mass of $\sim$2 keV, and behave as warm dark matter (WDM). This model is consistent with astrophysical and particle physics data, including constraints on neutrino masses from the Lyman α forest (Boyarsky et al. 2009b).

To investigate this WDM model, we have resimulated one of the Aquarius N-body haloes (Aq-A) with the power spectrum suppressed at small scales, as expected in the WDM case. N-body simulations of galactic and cluster WDM haloes were first carried out in the early 2000s (Colín, Avila-Reese & Valenzuela 2000; Bode, Ostriker & Turok 2001; Knebe et al. 2002). These studies found that fewer subhaloes form than in the CDM case and that these tend to be less concentrated than their CDM counterparts. Qualitatively, we

find similar results but the conclusions of these early simulations are difficult to interpret because, as we shall see later, the sharp cut-off in the power spectrum gives rise to the formation of a large number of artificial haloes that are purely numerical in origin (Wang & White 2007). More recently, Macciò & Fontanot (2010) carried out new simulations of WDM models and found that the luminosity function of satellites can be reproduced in these models just as well as it can in the CDM case.

Our simulations have orders of magnitude higher resolution than previous ones, enough to investigate reliably the inner structure of the galactic subhaloes that are potential hosts of the dwarf satellites. Furthermore, we carry out convergence tests of our results and develop a method for distinguishing genuine WDM haloes from the spurious objects that inevitably form in simulations of this kind. We describe our simulations in Section 2, present our results in Section 3, and conclude in Section 4.

2 THE SIMULATIONS

To compare the properties of subhaloes in Milky Way mass haloes in CDM and WDM universes, we have assembled a sample of five high-resolution simulations of galactic mass haloes. All the simulations have the same basic cosmological parameters: in units of the critical density, a total matter density, $\Omega_m = 0.25$, and a cosmological constant, $\Omega_\Lambda = 0.75$. The linear power spectrum has a spectral index $n_s = 1$ and is normalized to give $\sigma_8 = 0.9$, with $H_0 = 100 h$ km s^{-1} Mpc$^{-1} = 73$ km s^{-1} Mpc^{-1} (Springel et al. 2008).[2]

We have taken two simulations from the Aquarius project described in Springel et al. (2008), both of the same halo, Aq-A, but of different resolution, corresponding to levels 2 and 3 in the notation of Springel et al. (2008). The higher resolution, level 2, simulation has more than a hundred million particles within r_{200}, the radius of a sphere about the halo centre, encompassing a mean density of 200 times the critical density. The level 3 simulation has 3.6 times fewer particles. In both cases, the mass of the halo within r_{200} is about 1.8×10^{12} M$_\odot$, which is consistent with the estimated mass of the Milky Way (Li & White 2008; Xue et al. 2008; Gnedin et al. 2010). The basic properties of these haloes are given at the top of Table 1. Substructures were identified using the SUBFIND algorithm (Springel et al. 2001) to find gravitationally bound subhaloes within them.

We created three WDM counterparts to the CDM haloes by running new simulations using the same code and numerical parameters as Springel et al. (2008) but with WDM initial conditions. The WDM initial conditions were created keeping the same phases and the same unperturbed particle positions as in the CDM case, but using a WDM matter power spectrum instead to scale the amplitudes of the fluctuations. The linear matter power spectrum for both the CDM and WDM simulations is shown in Fig. 1 with solid lines adopting an arbitrary normalization at large scales.

The WDM power spectrum has a strong cut-off at high wavenumbers due to the free streaming of the WDM particles. In an unperturbed universe at the present day, the typical velocities of WDM

---

[1] The circular velocity is given by $V = [GM(< r)/r]^{1/2}$, where M is the mass enclosed within radius r and G is the universal gravitational constant; the value of r at which the maximum of this function, V_{max}, occurs is denoted by r_{max}.

[2] Although this set of parameters is discrepant at about the 3σ level with the latest constraints from microwave background and large-scale structure data (Komatsu et al. 2011), particularly with the values of σ_8 and n_s, the differences are not important for our purposes. For example, Boylan-Kolchin et al. (2011) show that the structure of Aquarius subhaloes is statistically similar to that of subhaloes in the Via Lactea simulations which assume a value of $\sigma_8 = 0.74$, lower than that of Komatsu et al. (2011), and a spectral index of 0.95.

Table 1. Basic parameters of the simulations analysed in this paper. The top two simulations are taken from the Aquarius sample of CDM dark matter haloes published in Springel et al. (2008). The simulations are of a single halo, Aq-A, at different numerical resolutions. The bottom three are WDM counterparts to the CDM simulations, as described in the main text. Columns 2–5 give the particle mass (m_p), the radius of the sphere of density 200 times the critical density (r_{200}), the halo mass within r_{200} (M_{200}) and the number of subhaloes within the main halo (N_s). The smallest subhaloes, determined by SUBFIND, contain 20 particles.

Name	m_p (M$_\odot$)	r_{200} (kpc)	M_{200} (M$_\odot$)	N_s
Aq-A2	1.370×10^4	245.88	1.842×10^{12}	30177
Aq-A3	4.911×10^4	245.64	1.836×10^{12}	9489
Aq-AW2	1.370×10^4	242.87	1.775×10^{12}	689
Aq-AW3	4.911×10^4	242.98	1.778×10^{12}	338
Aq-AW4	3.929×10^5	242.90	1.776×10^{12}	126
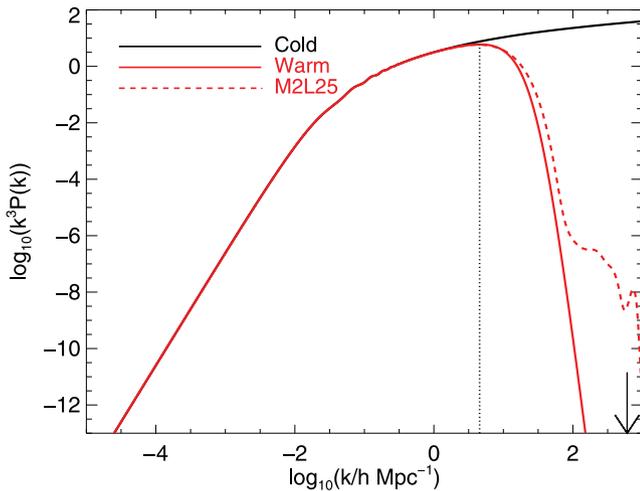
Figure 1. The solid lines show the linear power spectra (from CMBFAST; Seljak & Zaldarriaga 1996) used for the two simulations. Black is the original, CDM Aq-A spectrum, and red is that of Aq-AW. The vertical dashed line marks the peak of the WDM spectrum peak. The arrow marks the Nyquist frequency of the level 2 simulations. The dashed red curve corresponds to the M2L25 model of (Boyarsky et al. 2009b) which is almost identical to the solid red curve for scales below $k \sim 10 \, h \, \mathrm{Mpc}^{-1}$.

particles are only a few tens of m s^{-1}. This implies that the particles ceased to be relativistic after a redshift of $z \sim 10^7$, well before the end of the radiation-dominated era, as suggested by the word 'warm'. Fig. 2 illustrates the free streaming of a typical WDM particle over cosmic time. The area under the curve is the comoving distance travelled. It is evident that the WDM particle travels the greatest comoving distance during the radiation-dominated era after it has become non-relativistic (Bode et al. 2001). Over the duration of the N-body simulation, which starts at $z = 127$, a particle typically travels a distance of around 14 kpc, which is small compared to the total distance from early times of 400 kpc. For comparison, the mean interparticle separation for the high-resolution region in our highest resolution simulation is 7.4 kpc, similar to the free-streaming distance travelled by the particles after $z = 127$. This means that the effects of streaming during the simulation are small, and only affect scales that are barely resolved in our simulations. For this reason we chose to set the particle velocities in the same way as in the CDM case, where the particle velocity is a function of
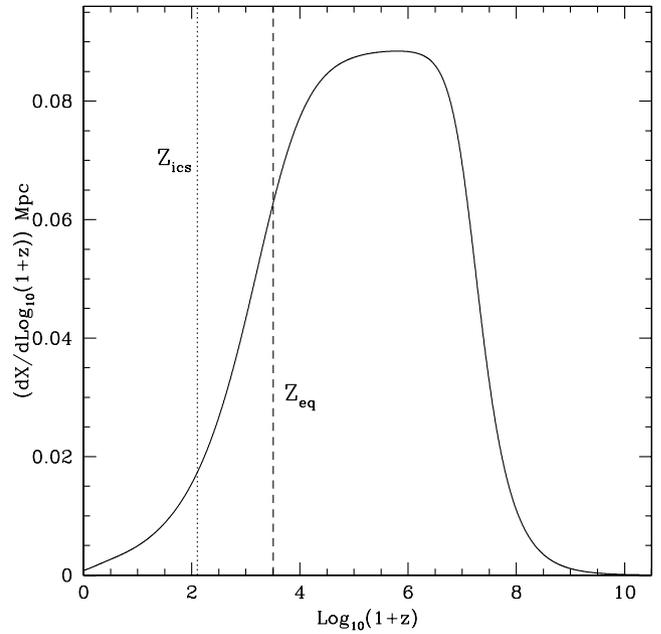
Figure 2. The free-streaming comoving distance travelled per log interval of $1 + z$, where z is redshift, for a WDM particle with a fiducial velocity of $24 \, \mathrm{m \, s}^{-1}$ at the present day. The dashed vertical line marks the redshift of matter–radiation equality. The dotted vertical line indicates the start redshift of the WDM simulations.

the unperturbed comoving position of a particle and is determined solely by the matter fluctuations.

The WDM matter power spectrum we assume has a shape characteristic of a 'thermal relic' (Bode et al. 2001). However, our WDM matter power spectrum is also an excellent fit for scales below $k \sim 10 \, h \, \mathrm{Mpc}^{-1}$, to the matter power spectrum of the M2L25 model of Boyarsky et al. (2009b), which is shown as a dashed line in Fig. 1. At $k = 10 \, h \, \mathrm{Mpc}^{-1}$, the power in both WDM curves is a factor 3 below that of CDM and falls away very rapidly beyond here in both models. The M2L25 model corresponds to a *resonantly produced* 2-keV sterile neutrino with a highly non-equilibrium spectrum of primordial velocities. The model is only just consistent with astrophysical constraints (Boyarsky et al. 2009b) and so maximizes the differences between the substructures in the CDM and WDM haloes, both in their internal structure and in their abundance.

For wavenumbers below the peak at $4.5 \, h \, \mathrm{Mpc}^{-1}$, the linear WDM power spectrum is well approximated by the product of the linear CDM power spectrum times the square of the Fourier transform of a spherical top-hat filter of unit amplitude and radius 320 kpc, or equivalently, containing a mass of $5 \times 10^9 \, \mathrm{M}_\odot$ at the mean density.

Images of the CDM and WDM haloes are shown in Fig. 3. As shown in Table 1, the mass of the main halo in the WDM simulation is very similar to that of the CDM halo, just a few per cent lighter. However, the number of substructures in the WDM case is much lower, reflecting the fact that the small-scale power in these simulations is greatly reduced. Some of the largest subhaloes can be matched by eye in the images of the two simulations.

Springel et al. (2008) showed that it is possible to make precise matches between substructures at different resolutions for the Aq-A halo, allowing the numerical convergence of properties of substructures to be checked for individual substructures. For this paper, we have found matches between subhaloes in the Aq-AW2, Aq-AW3 and Aq-AW4 simulations. We make these matches at the epoch when the subhaloes first have a mass which is more than half
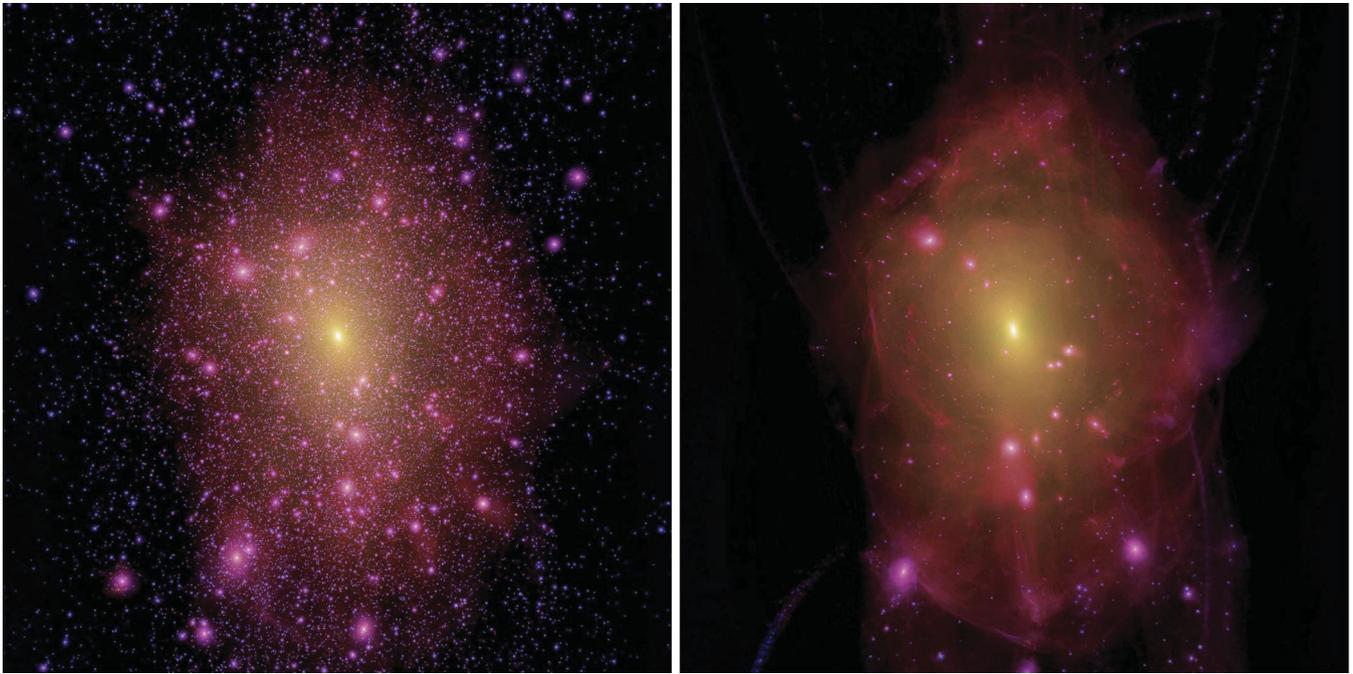
Figure 3. Images of the CDM (left) and WDM (right) level 2 haloes at $z = 0$. Intensity indicates the line-of-sight projected square of the density and hue the projected density-weighted velocity dispersion, ranging from blue (low velocity dispersion) to yellow (high velocity dispersion). Each box is 1.5 Mpc on a side. Note the sharp caustics visible at large radii in the WDM image, several of which are also present, although less well defined, in the CDM case.

the mass they have at the time when they first infall into the main halo (which is very close to the maximum mass they ever attain). At this epoch it is relatively easy to match the largest substructures in these three simulations as the corresponding objects have very similar positions, velocities and masses.

The number of subhaloes that can be matched between the two WDM simulations is much smaller than that between the corresponding CDM simulations, and is also a much smaller fraction of the total number of subhaloes identified by SUBFIND. The majority of substructures identified in the WDM simulations form through fragmentation of the sharply delineated filaments characteristic of WDM simulations and do not have counterparts in the simulations of different resolution. The same phenomenon is seen in hot dark matter simulations and is numerical in origin, occurring along the filaments on a scale matching the interparticle separation (Wang & White 2007). This artificial fragmentation is apparent in Fig. 3.

We will present a detailed description of subhalo matching in a subsequent paper but, in essence, we have found that matching subhaloes works best when comparing the Lagrangian regions of the initial conditions from which the subhaloes form, rather than the subhaloes themselves. We use a sample of the particles present in a subhalo at the epoch when it had half of the mass at infall to define the Lagrangian region from which it formed. We have devised a quantitative measure of how well the Lagrangian regions of the substructures overlap between the simulations of different resolution, and select as genuine only those subhaloes with strong matches between all three resolutions. We find that these criteria identify a sample of 15 relatively massive subhaloes with mass at infall greater than $2 \times 10^9 \, \mathrm{M}_\odot$, together with a few more subhaloes with infall mass below $10^9 \, \mathrm{M}_\odot$. This sample of 15 subhaloes includes all of the subhaloes with infall masses greater $10^9 \, \mathrm{M}_\odot$.

We have also found that the shapes of the Lagrangian regions of spurious haloes in our WDM simulations are typically very aspherical. We have therefore devised a second measure based on

sphericity as an independent way to reject spurious haloes. All 15 of the massive subhaloes identified by the first criterion pass our shape test, but all but one subhalo with an infall mass below $10^9 \, \mathrm{M}_\odot$ are excluded. For the purposes of this paper we need only the 12 most massive subhaloes at infall to make comparisons with the Milky Way satellites.

For both our WDM and CDM catalogues, we select a sample made up of the 12 most massive subhaloes at infall found today within 300 kpc of the main halo centre. In the Aq-AW2 simulation, these subhaloes are resolved with between about 2 and 0.23 million particles at their maximum mass. We use the particle nearest the centre of the gravitational potential to define the centre of each subhalo and hence determine the values of V_{max} and r_{max} defined in Section 1.

3 RESULTS

In this section, we study the central masses of the substructures found within 300 kpc of the centres of the CDM and WDM Milky Way like haloes. These results are compared with the masses within the half-light radii, inferred by Walker et al. (2009, 2010) and Wolf et al. (2010) from kinematic measurements, for the nine bright ($L_V > 10^5 \, \mathrm{L}_\odot$) Milky Way dwarf spheroidal galaxies.

Following the study by Boylan-Kolchin et al. (2011), in Fig. 4 we plot the correlation between V_{max} and r_{max} for the subhaloes in Aq-AW2 and Aq-A2 that lie within 300 kpc of the centre of the main halo. Only those WDM subhaloes selected using our matching scheme are included, whereas all Aq-A2 subhaloes are shown. The CDM subhaloes are a subset of those shown in fig. 2 of Boylan-Kolchin et al. (2011), and show V_{max} values that are typically ∼50 per cent larger than those of WDM haloes with a similar r_{max}. By assuming that the mass density in the subhaloes containing the observed dwarf spheroidals follows an NFW profile (Navarro, Frenk & White 1996b, 1997), Boylan-Kolchin et al. (2011) found
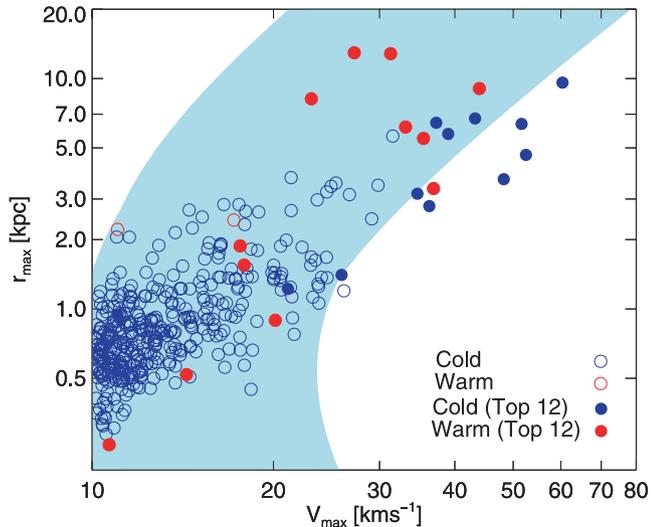
Figure 4. The correlation between subhalo maximum circular velocity and the radius at which this maximum occurs. Subhaloes lying within 300 kpc of the main halo centre are included. The 12 CDM and WDM subhaloes with the most massive progenitors are shown as blue and red filled circles, respectively; the remaining subhaloes are shown as empty circles. The shaded area represents the 2σ confidence region for possible hosts of the nine bright Milky Way dwarf spheroidals determined by Boylan-Kolchin et al. (2011).

Figure 5. Circular velocity curves for the 12 CDM (left) and WDM (right) subhaloes that had the most massive progenitors. The three red curves represent subhaloes with the most massive progenitors, which could correspond to those currently hosting counterparts of the LMC, SMC and the Sagittarius dwarf. The nine black curves might more fairly be compared with the data for the nine bright dwarf spheroidal galaxies of the Milky Way considered by Wolf et al. (2010). Deprojected half-light radii and their corresponding half-light masses, as determined by Wolf et al. (2010) from line-of-sight velocity measurements, are used to derive the half-light circular velocities of each dwarf spheroidal. These velocities and radii are shown as coloured points. The legend indicates the colour coding of the different galaxies.

the locus of possible (r_{max}, V_{max}) pairs that are consistent with the observed half-light radii and their enclosed masses. This is represented by the shaded region in Fig. 4. As Boylan-Kolchin et al. (2011) observed with their larger sample, several of the largest CDM subhaloes have higher maximum circular velocities than appears to be the case for the Milky Way bright dwarf spheroidals. By contrast, the largest WDM subhaloes are consistent with the Milky Way data.

Rather than assuming a functional form for the mass density profile in the observed subhaloes, a more direct approach is to compare the observed masses within the half-light radii of the dwarf spheroidals with the masses within the same radii in the simulated subhaloes. To provide a fair comparison, we must choose the simulated subhaloes that are most likely to correspond to those that host the nine bright dwarf spheroidals in the Milky Way. As stripping of subhaloes preferentially removes dark matter relative to the more centrally concentrated stellar component, we choose to associate final satellite luminosity with the maximum progenitor mass for each surviving subhalo. This is essentially the mass of the object as it falls into the main halo. The smallest subhalo in each of our samples has an infall mass of 3.2×10^9 M$_\odot$ in the WDM case, and 6.0×10^9 M$_\odot$ in the CDM case.

The LMC, SMC and the Sagittarius dwarf are all more luminous than the nine dwarf spheroidals considered by Boylan-Kolchin et al. (2011) and by us. As noted above, the Milky Way is exceptional in hosting galaxies as bright as the Magellanic Clouds, while Sagittarius is in the process of being disrupted so its current mass is difficult to estimate. Boylan-Kolchin et al. hypothesize that these three galaxies all have values of $V_{max} > 60$ km s^{-1} at infall and exclude simulated subhaloes that have these values at infall as well as $V_{max} > 40$ km s^{-1} at the present day from their analysis. In what follows, we retain all subhaloes but, where appropriate, we highlight those that might host large satellites akin to the Magellanic Clouds and Sagittarius.

The circular velocity curves at $z = 0$ for the 12 subhaloes which had the most massive progenitors at infall are shown in Fig. 5 for

both WDM and CDM. The circular velocities within the half-light radius of the nine satellites measured by Wolf et al. (2010) are also plotted as symbols. Leo-II has the smallest half-light radius, $\sim$200 pc. To compare the satellite data with the simulations, we must first check the convergence of the simulated subhalo masses within at least this radius. We find that the median of the ratio of the mass within 200 pc in the Aq-W2 and Aq-W3 simulations is W2/W3 $\sim$ 1.22, i.e. the mass within 200 pc in the Aq-W2 simulation has converged to better than $\sim$22 per cent.

As can be inferred from Fig. 5, the WDM subhaloes have similar central masses to the observed satellite galaxies, while the CDM subhaloes are almost all too massive at the corresponding radii. The CDM subhaloes have central masses that are typically 2–3 times larger than the Milky Way satellites. There is one CDM subhalo that lies at lower masses than all nine dwarf spheroidals, but this had one of the three most massive progenitors and has been almost completely destroyed by tidal forces.

Figs 4 and 5 show that the WDM subhaloes are less centrally concentrated than those in the corresponding CDM halo. Concentrations typically reflect the epoch at which the halo formed (Navarro et al. 1996b, 1997; Eke, Navarro & Steinmetz 2001). To investigate systematic differences in the formation epoch of the WDM and CDM subhaloes in our sample, we must choose a suitable definition of formation time. Since we are considering only the central mass, and we do not wish to introduce scatter in any correlation by using subhaloes that may have been stripped, we define the formation time as the first time at which the total progenitor mass exceeds the mass within 1 kpc at infall. The correlation of this redshift with the mass within 1 kpc at infall is shown in Fig. 6 for the 12 most massive WDM and CDM progenitors that survive to $z = 0$ as distinct subhaloes. Evidently, the proto-subhaloes that form later, which are generally WDM not CDM ones, have the lowest central
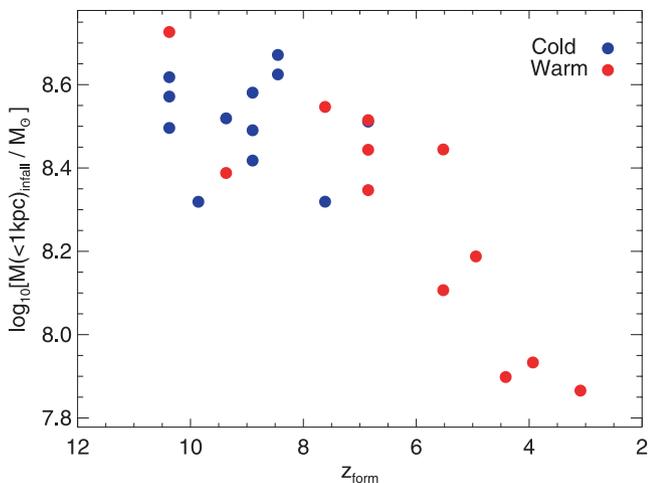
Figure 6. The correlation between subhalo central mass at infall and the redshift of formation, z_{form}, defined as the redshift at which the total mass of each proto-subhalo first exceeded this value. Central mass is defined within 1 kpc, and CDM and WDM results are shown with blue and red symbols, respectively.

masses. The mean difference between the top 12 WDM and CDM proto-subhalo masses within 1 kpc is approximately a factor 2.

Because of their later formation time, the infalling WDM subhaloes already have lower central masses than those falling into the corresponding CDM haloes. As their mass is less centrally concentrated, the WDM subhaloes are more susceptible to stripping. While this is most important in the outer regions of the subhaloes, the mass profiles in Fig. 5 show that the inner regions of some of the subhaloes have also endured significant depletion since infall. Fig. 7 shows, for both WDM and CDM subhaloes, the ratio, $M_{z=0}(<r)/M_{infall}$, of the present-day mass contained within $r = 0.5$, 1 and 2 kpc to the mass at infall, as a function of the central mass at infall at the chosen radius. On average, the median mass at infall for WDM is lower by ~ 0.15 dex than the corresponding

mass for CDM. One subhalo gains mass between infall and $z = 0$ because it accretes another subhalo. While there is a large scatter among the different subhaloes, with some having lost the majority of their central mass since infall, no significant systematic difference between WDM and CDM subhaloes is apparent. This implies that the reason why the WDM subhaloes provide a better fit to the half-light masses of the nine Milky Way dwarf spheroidals studied by Wolf et al. (2010) is not excess stripping but the later formation time, and correspondingly typical lower concentration, of the WDM proto-subhaloes compared to their CDM counterparts.

4 DISCUSSION AND CONCLUSIONS

The properties of the satellite galaxies of the Milky Way have posed a longstanding puzzle for CDM theories of galaxy formation. Two aspects of this puzzle have reportedly been separately and independently solved. One is the luminosity function of the satellites. The basic idea – the suppression of galaxy formation in small haloes by a combination of feedback effects produced by the reionization of gas at high redshift and supernova heating – was suggested by Kauffmann, White & Guiderdoni (1993) and explored thoroughly in the early 2000s (Bullock et al. 2000; Benson et al. 2002; Somerville 2002) and has been revisited many times since then (see Font et al. 2011, and references therein for the most recent discussion). The other aspect concerns the dynamical state of the satellites. Strigari et al. (2010) have shown that there exist subhaloes in the Aquarius CDM simulations that fit the stellar spectroscopic data for the well-studied satellites extremely well.

There is a third aspect to the puzzle, however, that has not yet been fully addressed and this is whether the CDM models that account for the satellite luminosity function also account for the satellites' internal dynamics. In other words, do the models assign the correct luminosities to subhaloes with the correct dynamics? At face value, the answer seems to be 'no'. This is already evident in the analysis of Strigari et al. (2010) in which the best-fitting dynamical models imply velocity dispersions (or equivalently V_{max} values) for the brightest dwarf spheroidals that are smaller than the velocity dispersions of the largest subhaloes. It is this discrepancy that has recently been highlighted by Boylan-Kolchin et al. (2011).

In this paper, we have compared a high-resolution N-body simulation of one of the Aquarius galactic haloes with a WDM counterpart. The initial conditions for both had the same phases and the same unperturbed particle positions. For the WDM simulation, we chose a form of the power spectrum corresponding to one of the models discussed by Asaka & Shaposhnikov (2005) and Boyarsky et al. (2009a), in which the dark matter is a sterile neutrino with mass ~ 2 keV, just consistent with various astrophysical constraints (Boyarsky et al. 2009b). The suppression of the power spectrum at masses below $\sim 10^{10}$ M$_\odot$ delays the formation of the haloes that will end up hosting the satellites and, as we have shown, this lowers their concentration compared to that of the corresponding CDM haloes. This is enough to reconcile the dynamics of the subhaloes with the data.

While a WDM model naturally produces haloes that are less concentrated than their CDM counterparts, this is only one possible solution to the puzzle. Other forms of dark matter such as 'meta-CDM' resulting from the decay of cold thermal relics could produce a similar outcome (Strigari, Kaplinghat & Bullock 2007). Also, it must be borne in mind that the values of V_{max} for Milky Way satellites are not directly measured but inferred by making assumptions about their dynamical state. If some of these assumptions are unrealistic, this could lead to an underestimate of the values of

Figure 7. The variation with subhalo mass at infall of the ratio of the present-day mass to the infall mass contained within 500 pc, 1 and 2 kpc. Data are shown for the 12 subhaloes identified at $z = 0$ which had the most massive progenitors, with CDM in blue and WDM in red. The symbol type denotes the radius interior to which the central mass is being measured, and large symbols show the medians of the corresponding distributions. We find no systematic differences between the CDM and WDM subhalo mass ratios.

V_{max} (e.g. Stoehr et al. 2002). Another possibility is that the satellite population of the Milky Way is not typical of the average to which the model predictions apply. It has recently been shown by Liu et al. (2011), Guo et al. (2011) and Lares et al. (2011) that the bright end of the Milky Way satellite luminosity function is different from the average. Finally, we cannot exclude the possibility that baryonic processes occurring during the formation of satellite galaxies in the CDM cosmogony might have lowered the concentration of haloes, for example, in the manner suggested by Navarro, Eke & Frenk (1996a). Recent simulations (Read & Gilmore 2005; Mashchenko, Wadsley & Couchman 2008; Governato et al. 2010) suggest that these processes could be important although it remains to be seen if they are enough to reconcile the CDM model with the dynamics of the Milky Way satellites.

REFERENCES

Asaka T., Shaposhnikov M., 2005, Phys. Lett. B, 620, 17
Benson A. J., Frenk C. S., Lacey C. G., Baugh C. M., Cole S., 2002, MNRAS, 333, 177
Bode P., Ostriker J. P., Turok N., 2001, ApJ, 556, 93
Boyarsky A., Ruchayskiy O., Shaposhnikov M., 2009a, Annu. Rev. Nuclear Particle Sci., 59, 191
Boyarsky A., Lesgourgues J., Ruchayskiy O., Viel M., 2009b, Phys. Rev. Lett., 102, 201304
Boylan-Kolchin M., Bullock J. S., Kaplinghat M., 2011, MNRAS, 415, L40
Bullock J. S., Kravtsov A. V., Weinberg D. H., 2000, ApJ, 539, 517
Busha M. T., Wechsler R. H., Behroozi P. S., Gerke B. F., Klypin A. A., Primack J. R., 2011, ApJ, 743, 117
Clocchiatti A. et al., 2006, ApJ, 642, 1
Cole S. et al., 2005, MNRAS, 362, 505
Colín P., Avila-Reese V., Valenzuela O., 2000, ApJ, 542, 622
Davis M., Efstathiou G., Frenk C. S., White S. D. M., 1985, ApJ, 292, 371
Eke V. R., Navarro J. F., Steinmetz M., 2001, ApJ, 554, 114
Font A. S. et al., 2011, MNRAS, 417, 1260
Gnedin O. Y., Brown W. R., Geller M. J., Kenyon S. J., 2010, ApJ, 720, L108
Governato F., et al., 2010, Nat, 463, 203
Guo Q., Cole S., Eke V., Frenk C., 2011, MNRAS, 417, 370
Guy J. et al., 2010, A&A, 523, A7
Kauffmann G., White S. D. M., Guiderdoni B., 1993, MNRAS, 264, 201
Klypin A., Kravtsov A. V., Valenzuela O., Prada F., 1999, ApJ, 522, 82
Knebe A., Devriendt J. E. G., Mahmood A., Silk J., 2002, MNRAS, 329, 813
Komatsu E. et al., 2011, ApJS, 192, 18
Lares M., Lambas D. G., Domínguez M. J., 2011, AJ, 142, 13
Li Y., White S. D. M., 2008, MNRAS, 384, 1459
Liu L., Gerke B. F., Wechsler R. H., Behroozi P. S., Busha M. T., 2011, ApJ, 733, 62
Macciò A. V., Fontanot F., 2010, MNRAS, 404, L16
Madau P., Diemand J., Kuhlen M., 2008, ApJ, 679, 1260
Mashchenko S., Wadsley J., Couchman H. M. P., 2008, Sci, 319, 174
Moore B., Ghigna S., Governato F., Lake G., Quinn T., Stadel J., Tozzi P., 1999, ApJ, 524, L19
Navarro J. F., Eke V. R., Frenk C. S., 1996a, MNRAS, 283, L72
Navarro J. F., Frenk C. S., White S. D. M., 1996b, ApJ, 462, 563
Navarro J. F., Frenk C. S., White S. D. M., 1997, ApJ, 490, 493
Read J. I., Gilmore G., 2005, MNRAS, 356, 107
Seljak U., Zaldarriaga M., 1996, ApJ, 469, 437
Somerville R. S., 2002, ApJ, 572, L23
Springel V., White S. D. M., Tormen G., Kauffmann G., 2001, MNRAS, 328, 726
Springel V. et al., 2008, MNRAS, 391, 1685
Stoehr F., White S. D. M., Tormen G., Springel V., 2002, MNRAS, 335, L84
Strigari L. E., Kaplinghat M., Bullock J. S., 2007, Phys. Rev. D, 75, 061303
Strigari L. E., Frenk C. S., White S. D. M., 2010, MNRAS, 408, 2364
Walker M. G., Mateo M., Olszewski E. W., Peñarrubia J., Wyn Evans N., Gilmore G., 2009, ApJ, 704, 1274
Walker M. G., Mateo M., Olszewski E. W., Peñarrubia J., Wyn Evans N., Gilmore G., 2010, ApJ, 710, 886
Wang J., White S. D. M., 2007, MNRAS, 380, 93
Wolf J., Martinez G. D., Bullock J. S., Kaplinghat M., Geha M., Muñoz R. R., Simon J. D., Avedo F. F., 2010, MNRAS, 406, 1220
Xue X. X. et al., 2008, ApJ, 684, 1143

This paper has been typeset from a TeX/LaTeX file prepared by the author.